Journal of Colloid and Interface Science 582 (2021) 1203–1212

Contents lists available at ScienceDirect

Journal of Colloid and Interface Science

journal homepage: www.elsevier.com/locate/jcis

Regular Article

Filtration and removal of liquid polymers from water (polymer/water separation) by use of the underwater superpolymphobic mesh produced with a femtosecond laser

Jiale Yong [a,c], Xue Bai [a,c], Qing Yang [b,*], Xun Hou [a], Feng Chen [a,c,*]

[a] State Key Laboratory for Manufacturing System Engineering and Shaanxi Key Laboratory of Photonics Technology for Information, School of Electronic Science and Engineering, Xi'an Jiaotong University, Xi'an 710049, PR China
[b] School of Mechanical Engineering, Xi'an Jiaotong University, Xi'an 710049, PR China
[c] The International Joint Research Laboratory for Micro/Nano Manufacturing and Measurement Technologies, Xi'an Jiaotong University, Xi'an 710049, PR China

HIGHLIGHTS

- The mixture of polymer and water is separated by underwater superpolymphobic meshes.
- Underwater superpolymphobicity is achieved on the mesh by fs laser processing.
- The structured mesh has excellent repellence to liquid polymer in water.
- The separation can alleviate pollution caused by the discharge of liquid polymers.

GRAPHICAL ABSTRACT

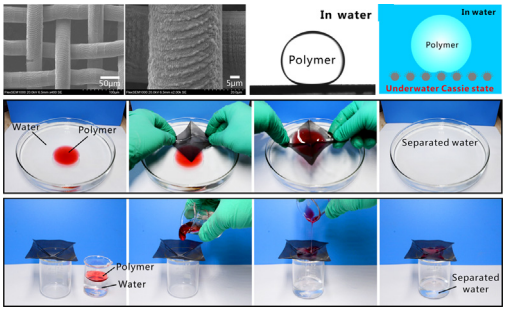

ARTICLE INFO

Article history:
Received 7 July 2020
Revised 3 September 2020
Accepted 3 September 2020
Available online 8 September 2020

Keywords:
Polymer/water separation
Underwater superpolymphobicity
Femtosecond laser
Superhydrophilicity
Liquid polymer
Metal mesh

ABSTRACT

The widespread use of liquid polymers may pollute water, causing grave environmental problems and even various human diseases. The separation of a mixture of a liquid polymer and water is extremely important in research, but the high viscosity, low fluidity, and high adhesion performance of liquid polymers make this task highly challenging. In this paper, we propose a novel strategy for separating a polymer/water mixture wherein porous underwater superpolymphobic micro/nanostructures are used for the first time. Femtosecond laser (fsL) processing is used to form micro/nanoscale surface structures on a stainless steel mesh (SSM), resulting in excellent repellence (underwater superpolymphobicity) to various liquid polymer droplets in water. The laser-induced underwater superpolymphobicity is very stable even though the SSM suffers from different damage treatments (e.g., sandpaper abrasion, acid or alkali solutions corrosion, UV light irradiation, and tape peeling). The underwater superpolymphobicity is ascribed to an underwater Cassie contact state between the underwater liquid polymer and the surface microstructure of the laser-treated SSM. We demonstrate that the underwater superpolymphobic SSM can be effectively and repeatedly used to separate liquid polymer/water mixtures with a high separation efficiency of 99.0% and a high separation flux of 4.45×10^5 L $m^{-2}h^{-1}$. The mixtures of water and different polymers are successfully separated. Such a separation strategy can potentially alleviate pollution from liquid polymer discharge, recycle waste polymer resources, and be applied in polymer production and manufacturing.

* Corresponding authors at: State Key Laboratory for Manufacturing System Engineering and Shaanxi Key Laboratory of Photonics Technology for Information, School of Electronic Science and Engineering, Xi'an Jiaotong University, Xi'an 710049, PR China (F. Chen).
E-mail addresses: yangqing@xjtu.edu.cn (Q. Yang), chenfeng@mail.xjtu.edu.cn (F. Chen).

https://doi.org/10.1016/j.jcis.2020.09.010
0021-9797/

1. Introduction

The separation of two or more dissimilar materials has important implications for both fundamental research and practical applications [1–10]. Polymers are commonly used materials that exhibit both liquid and solid states with a broad range of applications in the chemical industry, building, food processing, pharmaceuticals, agriculture, etc. However, the widespread use of liquid polymers results in various pollutants in water [11–16]. The leakage and discharge of liquid polymers into the water in the abovementioned applications may cause waste and even polymer-based environmental problems. A liquid polymer is generally characterized by high viscosity, low fluidity, and high adhesion performance. Liquid polymer pollutants can easily adhere to and block underwater pipelines and facilities. These pollutants are typically difficult to biodegrade using microbes in water. The entrance of toxic compounds in liquid polymers into the food chain constitutes a significant threat to the ecosystem and can cause various human diseases (e.g. cancer) [11–16]. Pollution caused by waste liquid polymers can be potentially remedied by separating liquid polymer/water mixtures. However, liquid polymers can easily adhere to commonly used separation materials and are difficult to isolate from water. An effective separation method for minimizing the negative impact of liquid polymer pollution has not been available thus far. The polymer/water separation can be defined as the process of separating a mixture of water and liquid polymers. The development of a simple and effective strategy for polymer/water separation has considerable research significance but is highly challenging to accomplish.

We recently reported several solid surfaces that have a high capacity to repel a liquid polymer in a water medium; that is, liquid polymer droplets on the sample surfaces have a contact angle (CA) above 150°, and the sample surface exhibits ultralow adhesion to a polymer in water [17–19]. This property is defined as underwater superpolymphobicity by us. Underwater superpolymphobicity has been successfully used to design the shape of polymers and control the adhesion at polymer/substrate interfaces. The excellent polymer repellence of underwater superpolymphobic materials can be used in polymer/water separation to mitigate liquid-polymer-induced waste and environmental pollution. To the best of our knowledge, the use of a polymer-repellent microstructure to separate a polymer/water mixture has not been reported thus far.

The femtosecond (10^{-15}s) laser (fsL) has become one of the most advanced tools in the field of micro/nano-fabrication because of its extremely short pulse width and ultrahigh peak power density [20–26]. Femtosecond laser microfabrication possesses many unique features, such as small heat-affected area, high spatial resolution, a wide range of processable materials, and non-contact processing [20–26]. A femtosecond laser can process almost any given materials and can directly produce micro- and nano-scale structures on the material surface by simple one-step ablation. In this paper, micro/nanostructures were fabricated on a stainless steel mesh (SSM) surface by one-step fsL processing. The resultant SSM exhibits superhydrophilicity and high repellence to various liquid polymers in water. The underwater superpolymphobicity results from the Cassie contact state between the liquid polymer and the fsL-treated SSM, which is verified by scanning electronic microscope (SEM) imaging. The influence of processing parameters on the polymer wettability of the treated SSM was also investigated. The sandpaper abrasion, acid or alkali solutions corrosion, UV light irradiation, and tape peeling experiments were carried out to show the durability of the laser-induced underwater superpolymphobicity. Based on the inverse wettabilities of the fsL-structured SSM to water (i.e. superhydrophilicity in the air) and the liquid polymer (i.e. underwater superpolymphobicity), we propose a novel strategy for separating a polymer/water mixture, wherein porous underwater superpolymphobic micro/nanostructures are used for the first time. Different mixtures of liquid polymer and water were successfully separated by the fsL-structured SSM using both removal and filtration.

2. Results and discussion

FsL processing was adopted to generate a microstructure on an SSM surface. As shown in Fig. 1, the SSM (300 mesh size) was fixed on a movable platform controlled by a program. The fsL beam (pulse width = 50 fs, center wavelength = 800 nm, and repetition rate = 1 kHz) was focused on the SSM surface by a convex lens (focal length = 20 cm), and the SSM was ablated using a line-by-line progressive scanning technology (inset of Fig. 1) [27–36]. The laser power and the scanning speed were set at constant values of 300 mW and 5 mm s^{-1}, respectively. The interval, Λ, between adjacent scanning lines was changed during fsL processing.

Fig. 2a is an SEM image of the wire surface of an untreated bare SSM. The surface of the SSM is relatively smooth, and only the inherent texture of the metal wire can be observed. By contrast, fsL treatment easily creates a rough microstructure on the SSM surface. Fig. 2b is an SEM image of the fsL-structured SSM at the Λ of 25 μm. A wave-like microstructure is generated on the wire surface. This microstructure is composed of microscale (0.5–2 μm) protuberances and typical nanoscale fsL-induced ripples. Increasing Λ from 25 μm to 75 μm still results in a wave-like hierarchical microstructure on the SSM surface (Fig. 2b-d). For Λ above 75 μm, the resultant SSM surface is coated with only periodic nanoripples with a period of approximately 625 nm (Fig. 2e and f). Generally, the fsL energy accumulation per unit area decreases with increasing Λ, and a lower energy accumulation weakens the ablation process. Therefore, the scale of the fsL-induced surface micro/nanostructures gradually declines as Λ increases (Fig. 2).

Fig. 3 shows the X-ray diffraction (XRD) patterns of the SSM before and after fsL ablation, which was performed to further study the chemical changes of the sample surface. These two patterns have the same peak positions. The result indicates that the chemical composition of the SSM almost does not change during laser ablation although oxidation occurs under fsL ablation [37].

The original untreated SSM is silver-gray (Fig. 4a). A water droplet on this SSM has a water CA (WCA) of 101.9 ± 13.5° (Fig. 4c). The untreated SSM exhibits polymphilicity. The polymer CA

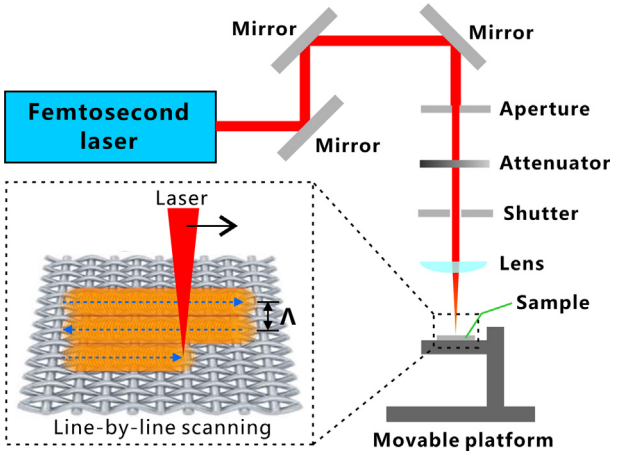

Fig. 1. Schematic of setup for ablating SSM by focused fsL beam.

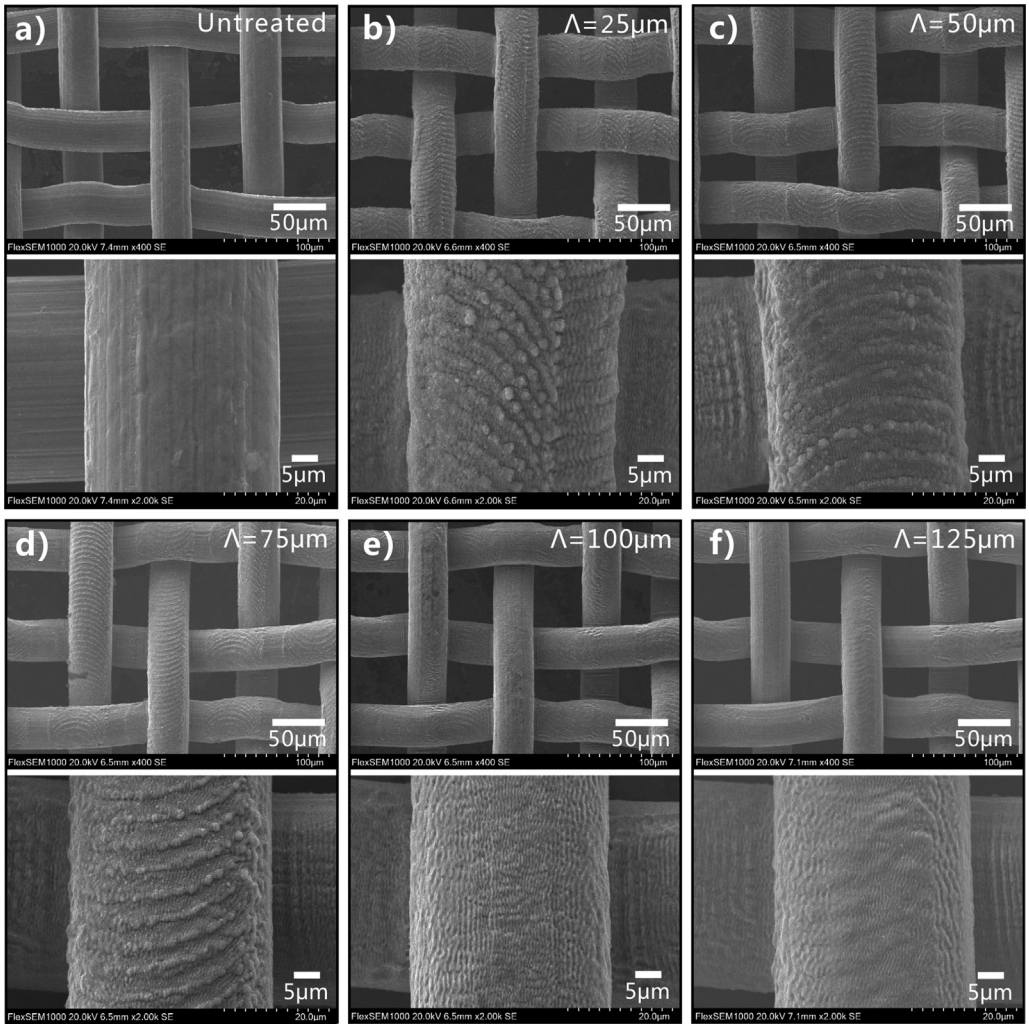

Fig. 2. SEM images of SSM surfaces. (a) Untreated SSM. (b-f) SSM following fsL treatment at different scanning intervals of (b) Λ = 25 μm, (c) Λ = 50 μm, (d) Λ = 75 μm, (e) Λ = 100 μm, and (f) Λ = 125 μm.

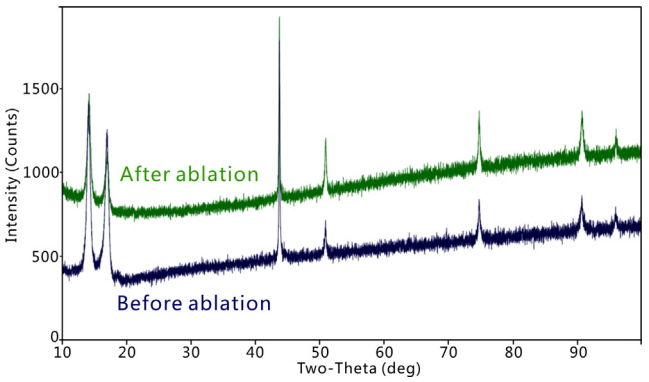

Fig. 3. XRD patterns of the SSM before and after fsL ablation.

(PCA) of liquid polymer (uncured polydimethylsiloxane (PDMS)) droplets on the SSM is only 23.2 ± 7.9° (Fig. 4d). Immersion in water makes the SSM polymphobic. The PCA of an underwater polymer droplet on the untreated SSM is measured to be 143.5 ± 2.0° (Fig. 4e). Despite the large PCA, there is very strong adhesion between the untreated SSM and the polymer droplet. The underwater polymer droplet adheres to the SSM, irrespective of any tilting angles of the SSM (inset of Fig. 4e). After roughening by fsL processing (e.g., Λ = 75 μm), the SSM surface becomes black because of the formation of light-absorbing micro/nanoscale structures (Fig. 4b). The structured SSM exhibits superhydrophilicity and superpolymphilicity in air. A water droplet and a liquid polymer droplet fully wet the SSM with a WCA and a PCA, respectively, near 0° (Fig. 4f and g). By contrast, a liquid polymer droplet dispensed on the structured SSM in water maintains a spherical shape with a PCA of 156.4 ± 5.1° (Fig. 4h). As long as the SSM is tilted at 2.5 ± 0.5°, the polymer droplet rolls off the surface easily (Fig. 4i and Movie S1); that is, the polymer sliding angle (PSA) equals 2.5 ± 0.5°. The CA hysteresis (CAH) of the underwater polymer droplet on the SSM is only 2.7 ± 2°. Therefore, the structured SSM exhibits high repellence to liquid polymer droplets in water. The high PCA (>150°) and low PSA/CAH (<10°) demonstrate that the fsL treatment has endowed the SSM with underwater superpolymphobicity.

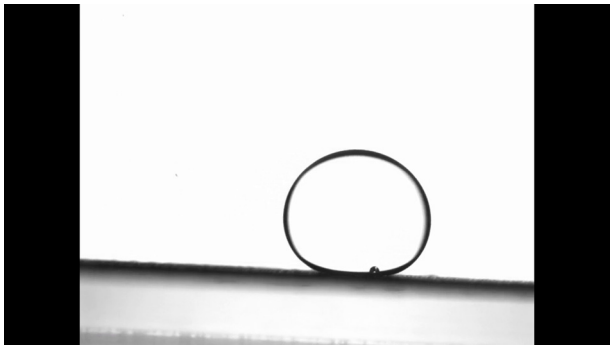

Movie S1.

The wettability of a liquid polymer droplet on different kinds of SSMs was also investigated by a dynamic contacting-leaving process. As shown in Fig. 5, a needle was used to place a liquid polymer droplet in contact with the SSM surface. After an appropriate contact period, the droplet was moved away from the SSM. For the untreated SSM, the polymer droplet eventually detached from the needle as the needle was lifted in both air (Fig. 5a and Movie S2) and water (Fig. 5b and Movie S2). The shape of the polymer droplet deformed drastically before detaching from the needle. The polymer droplet adhered easily to the untreated SSM, demonstrating the ultrahigh adhesion between the SSM and the liquid polymer. By contrast, the polymer droplet maintained a spherical shape during the entire process (from contacting the laser-structured SSM to removal by the needle), and no residual was left on the underwater superpolymphobic SSM surface (Fig. 5c and Movie S2). This result shows that the fsL-structured SSM exhibits remarkable repellence to polymer in water.

Fig. 6 depicts the influence of Λ on the wettability of the laser-structured SSM. With increasing Λ, the focused laser pulses per area decline, weakening the ablation process and decreasing the roughness. The WCA between the resulting SSM and a water droplet increases gradually with increasing Λ because the laser-ablated domains at the scanning lines develop from an overlapped state into a separated state (Fig. 6a), which is in good agreement with previously reported results [28,38]. All the laser-structured SSMs with $\Lambda < 100$ μm exhibit excellent superhydrophilicity, with WCAs below 10°. With increasing Λ, the PCA of an underwater polymer droplet decreases, whereas the CAH increases (Fig. 6b). As the Λ increases from 25 μm to 175 μm, the PCA decreases from 155.8 ± 1.8° to 151.2 ± 3.2°, and the CAH increases from 2.8 ± 0.9° to 14.6 ± 1.7°. This result shows that underwater superpolymphobicity can be obtained on a laser-treated SSM over a wide range of processing parameters.

The real contact state between the underwater liquid polymer and the structured SSM is estimated by performing SEM imaging after curing the PDMS at a high temperature. Fig. 7a and b show liquid polymer poured onto an untreated SSM in air. The SEM images show that the polymer fully wets the SSM. All the SSM holes are filled with polymer. The liquid polymer is in a Wenzel

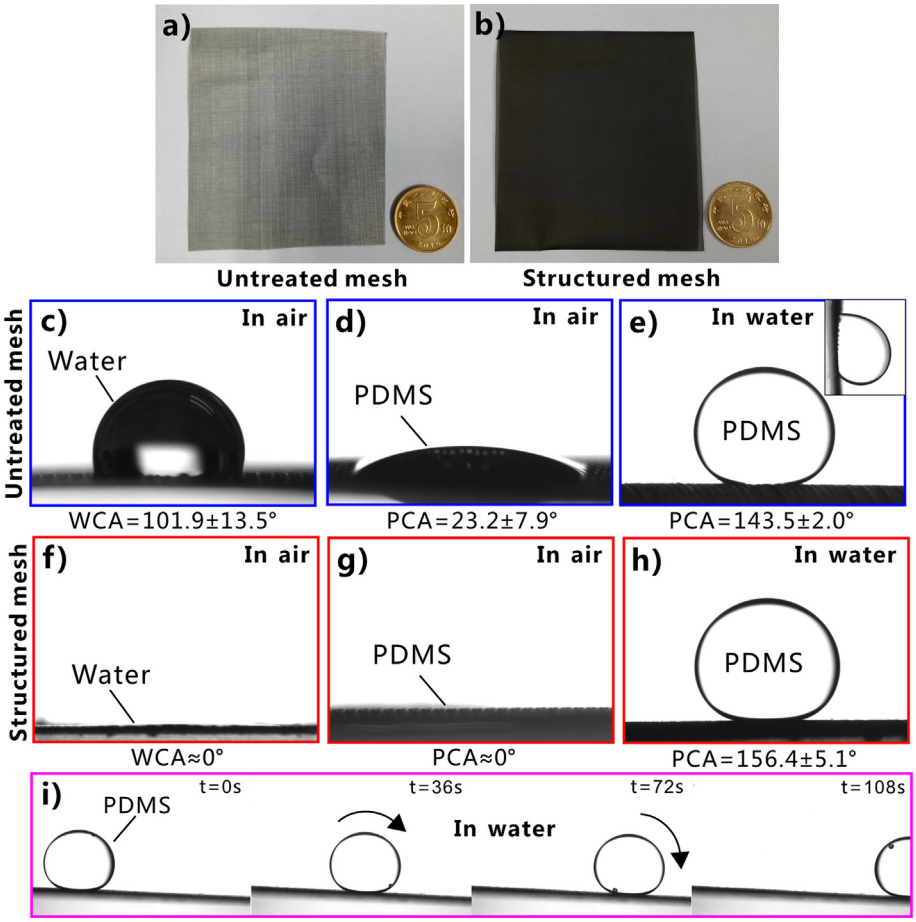

Fig. 4. SSM wettability. (a) Photograph of the untreated SSM. (b) Photograph of the SSM after fsL processing. (c and f) Water wettability of SSM in air. (d and g) Liquid polymer droplet on SSM in air. (e and h) Underwater liquid polymer droplet on SSM. (c-e) show the untreated SSM and (f-h) show the laser-structured SSM. Inset in (e) shows that polymer droplet sticks firmly to a 90°-tilted SSM. (i) Liquid polymer droplet rolling off the structured SSM underwater.

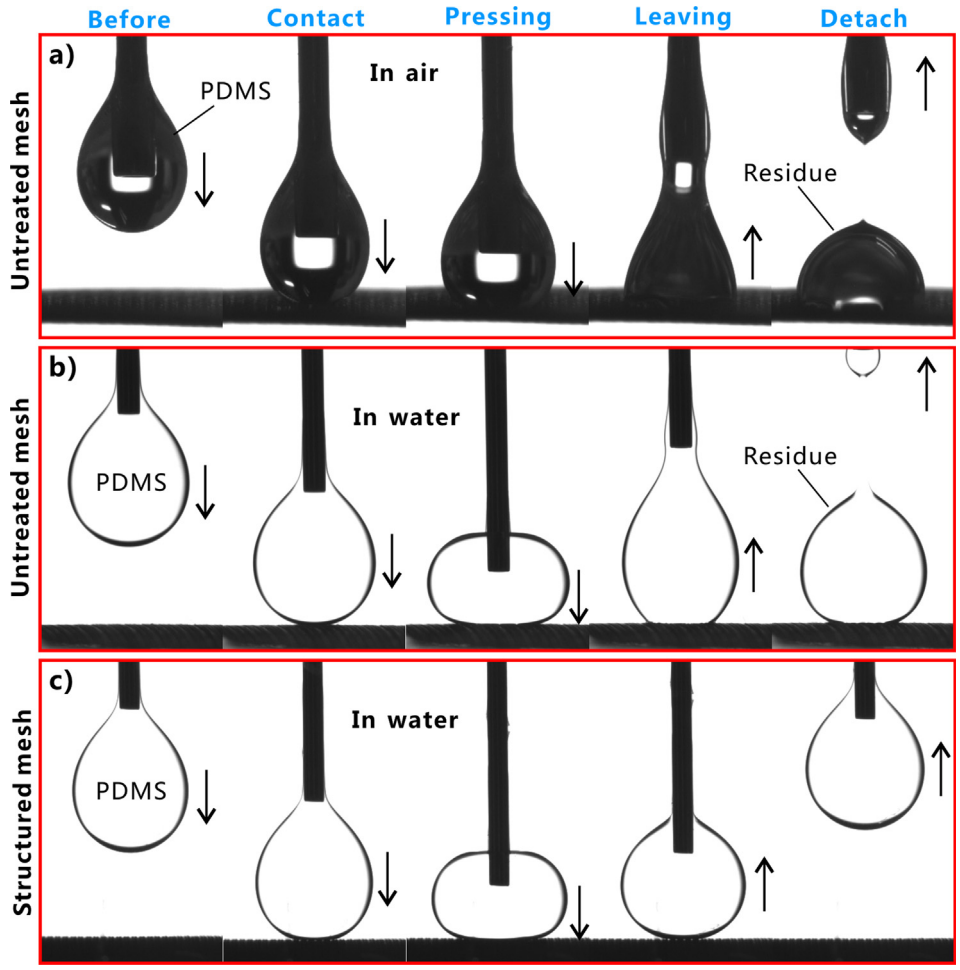

Fig. 5. Process of placing an underwater polymer droplet in contact with and removal from SSM. (a) Untreated SSM in air. (b) Untreated SSM in water. (c) Laser-structured SSM in water.

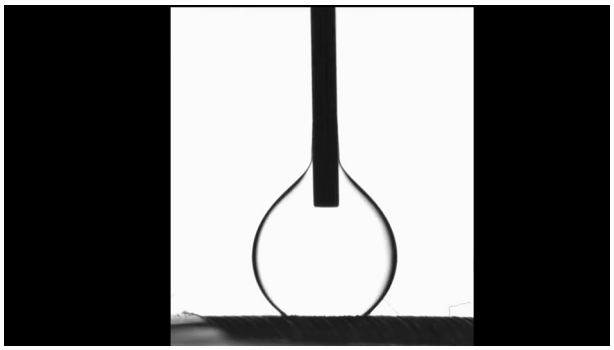

Movie S2.

state on the untreated SSM (Fig. 7c) [38,39]. For the laser-structured SSM, the SEM images show that underwater polymer remains a spherical shape on the SSM surface and only contacts the top portion of the SSM microstructure (Fig. 7d and e). The polymer droplet on the rough SSM in water is an underwater Cassie wetting state (Fig. 7f) [39–41]. The rough surface microstructure generated by laser ablation amplifies the wettability of SSM, resulting in superhydrophilicity. The structured SSM is completely wetted when immersed in water. The water fills all the SSM holes and surface microstructures. Placing a polymer droplet on the underwater SSM results in the formation of a water cushion between the laser-induced microstructure and the polymer droplet [41]. The trapped water layer repels the liquid polymer because of the repulsive force between water and polymer molecules. As a result, the structured SSM is endowed with excellent polymer repellence in water, i.e., underwater superpolymphobicity.

The underwater superpolymphobicity of the laser-structured SSM is very robust and the durability is critical for its practical applications. Fig. 8a shows the PCA and CAH values of an underwater polymer droplet on the resultant mesh that is damaged by different cycles of sandpaper abrasion. It is demonstrated that the PCA and CAH values almost have no obvious change with increasing abrasion times. Even after 50 cycles of sandpaper abrasion, the mesh still maintained great repellence to polymer droplets in water, revealing the strong abrasion-resistant ability of the underwater superpolymphobic mesh. When the laser-structured mesh was immersed in the solutions with different pH for 12 h, the mesh still had underwater superpolymphobicity with PCA above 150° and CAH below 10° (Fig. 8b). Therefore, the laser-induced underwater superpolymphobic mesh has remarkable chemical resistance and anti-corrosion ability. The mesh also can withstand long-time UV irradiation. The underwater superpolymphobicity is almost uninfluenced after irradiating the mesh by UV light for 24 h (Fig. 8c). Fig. 8d shows the wettability of the structured mesh after the tape peeling test. The PCA of the treated mesh always remains above 150° with increasing cycles of tape peeling to 50. However, the CAH increases with the increase of the tape peeling cycles. The increased adhesion between the treated mesh and polymer droplet is ascribed to that the adhesive matter on tape adheres

to the mesh surface. The underwater superpolymphobicity with low adhesion to polymer droplet can be obtained within 40 tape peeling cycles. Such stability of underwater superpolymphobicity benefits from the inherent chemical inertness and hardness of the stainless steel substrate and the laser-induced surface microstructures.

The inverse wettabilities of the laser-structured SSM to water (i.e., superhydrophilicity) and the polymer (i.e. underwater superpolymphobicity) enable the SSM to separate the polymer/water mixture. The structured SSM was successfully used as a separation medium for a mixture of liquid polymer and water. Fig. 9a and Movie S3 show the removal/collection of liquid PDMS floating on the water surface. This case corresponds to a small liquid polymer (red) leaked in water (Fig. 9a-1). The laser-structured SSM was previously wetted by water. The wetted SSM was submerged in water (Fig. 9a-2) and placed beneath the polymer layer (Fig. 9a-3). The SSM was then pulled up similar to a fishing net (Fig. 9a-4). The liquid polymer remained on the as-prepared SSM and was therefore removed from the water surface (Fig. 9a-5). Fig. 9b and Movie S4 shows the process of separating the polymer/water mixture by

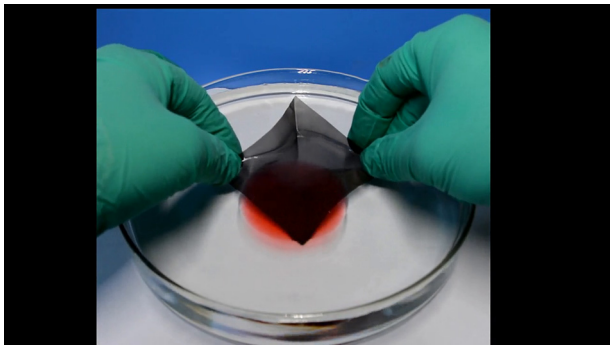

Movie S3.

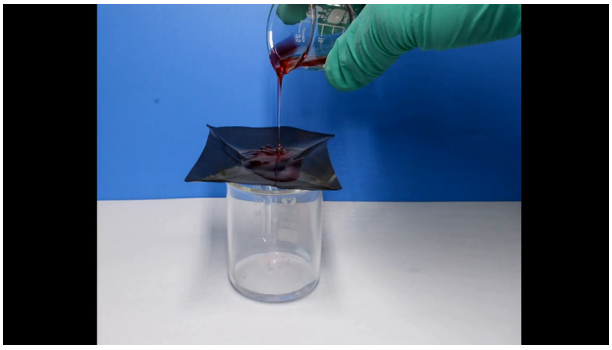

Movie S4.

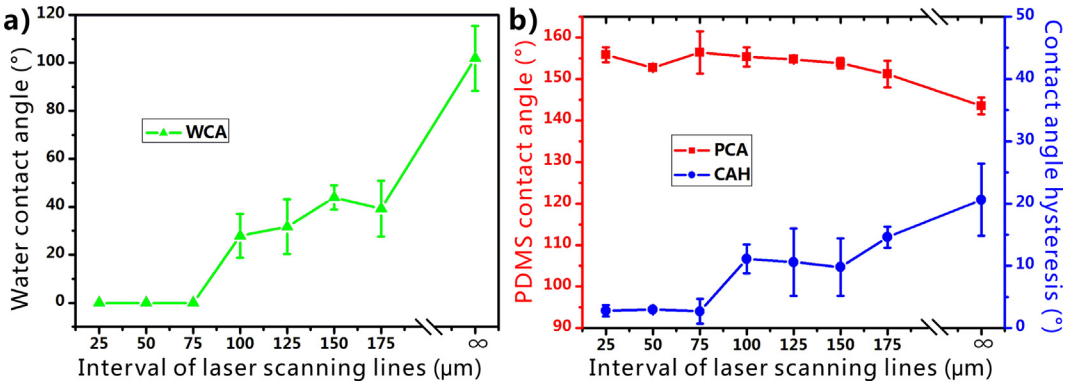

Fig. 6. Influence of Λ on the wettability of the laser-ablated SSM. (a) Water wettability in air. (b) Underwater wettability of a liquid polymer droplet.

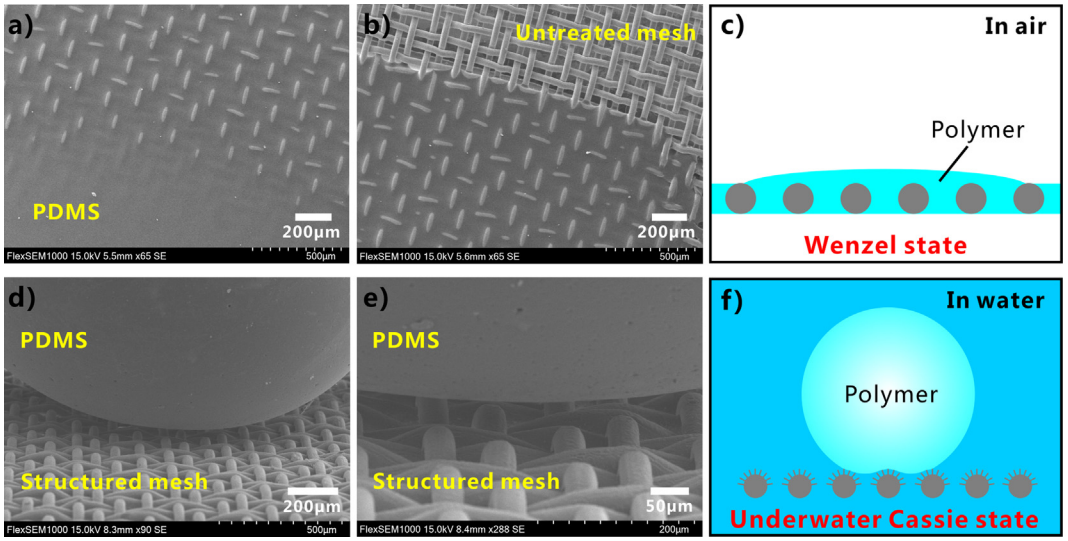

Fig. 7. Wetting state between liquid polymer and SSM. (a and b) SEM images of polymer on the untreated SSM. (c) Schematic of liquid polymer droplet on the untreated SSM in air. (d and e) SEM images of a polymer droplet on the laser-structured SSM. (f) Schematic of liquid polymer droplet on the structured SSM in water. SEM images were obtained after curing the polymer (PDMS).

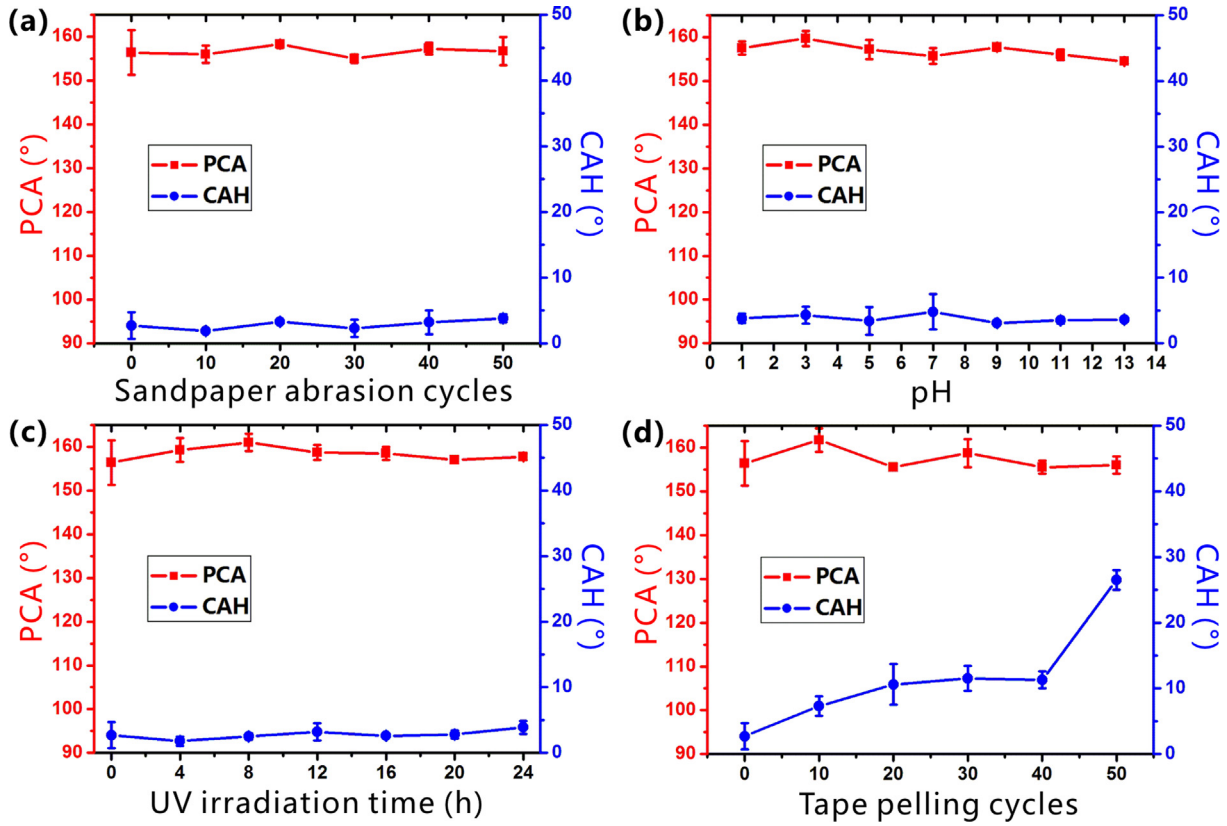

Fig. 8. Durability of the underwater superpolymphobicity of the laser-structured SSM. (a) After sandpaper abrasion. (b) After immersion in the acid or alkali solutions with different pH. (c) After UV light irradiation. (d) After tape peeling.

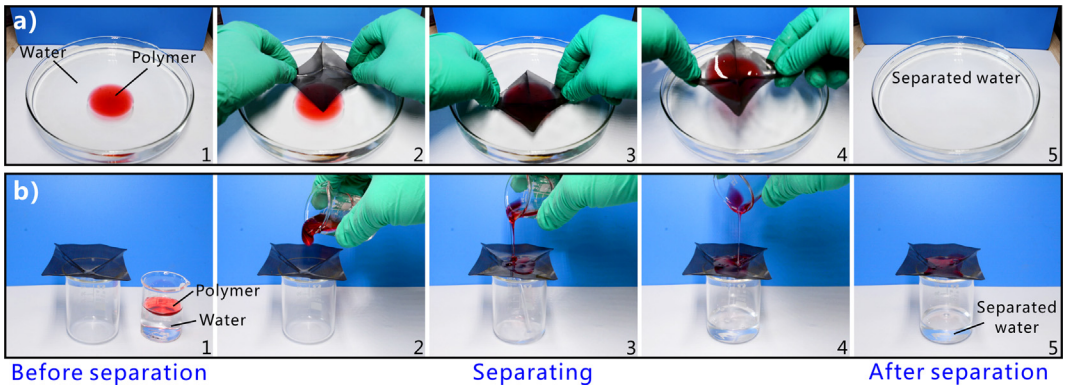

Fig. 9. Polymer/water separation by using laser-structured underwater superpolymphobic SSM as a separation medium. (a) Removal/collection of liquid polymer floating on the water surface. (b) Filtration of polymer/water mixture. The polymer is liquid PDMS dyed with Oil Red O. (For interpretation of the references to colour in this figure legend, the reader is referred to the web version of this article.)

filtration. A structured SSM was prewetted using a small volume of water and mounted on a beaker (Fig. 9b-1). The mixture of water and liquid polymer (red) was poured onto the SSM (Fig. 9b-2). The water in the mixture gradually penetrated through the structured SSM and dripped into the beaker below (Fig. 9b-3). By contrast, the liquid polymer was intercepted by the SSM because of the fsL-induced underwater superpolymphobicity and therefore always remained above the SSM (Fig. 9b-4). The separation process ended when all the water passed through the structured SSM (Fig. 9b-5). The polymer/water mixture was thus successfully separated. It is demonstrated that no polymer remained in the separated water for both removal and filtration observed under a microscope. The measured separation efficiency reaches up to 99.0%, showing that the fsL-treated SSM has a high separation efficiency. The rich pores and the superhydrophilicity enable the SSM to have an average separation flux of 4.45×10^5 L $m^{-2}h^{-1}$. The liquid polymer on the SSM surface can be easily cleaned or collected because of the excellent polymer repellence of the structured SSM. Repeatability is important for such separation material in practical application [42,43]. The cleaned SSM can be repeatedly used to separate the polymer/water mixture. Even after 10 cycles of separation, the cleaned SSM still maintained its underwater superpolymphobicity and separation ability, benefiting from the stability of underwater superpolymphobicity of the laser-structured SSM. This result demonstrates that the structured SSM was not contaminated by liquid polymer during the entire separation process, because the

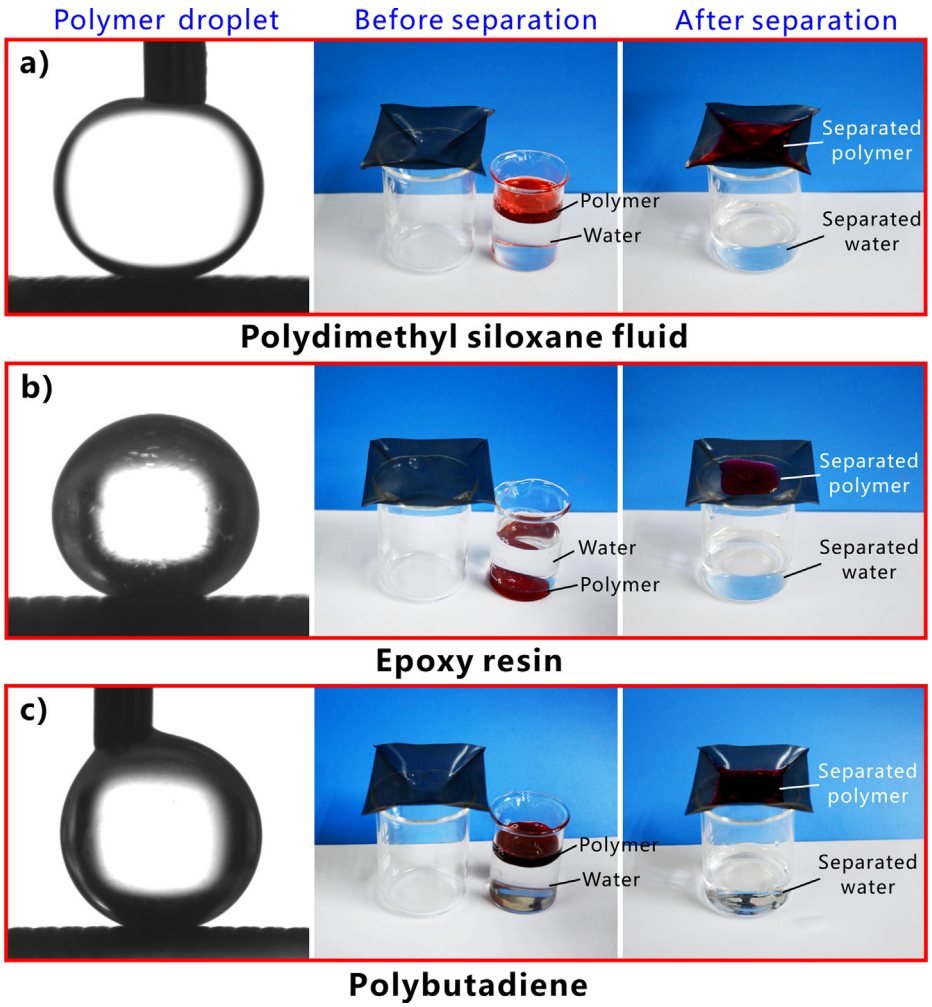

Fig. 10. Separating different polymer/water mixtures by the laser-induced underwater superpolymphobic SSM. The used polymer in (a) is polydimethyl siloxane fluid, that in (b) is epoxy resin, and that in (c) is polybutadiene. First column: the polymer droplet on the SSM in water. Second column: the polymer/water mixture before separation. Third column: after separation.

liquid polymer could not effectively contact the surface microstructures of the underwater superpolymphobic SSM. By contrast, when an untreated SSM is used to perform the separation experiment, both water and liquid polymer pass through the mesh, and the polluted mesh is difficult to clean.

In addition to liquid PDMS droplets, the laser-structured SSM also shows remarkable underwater superpolymphobicity to a broad range of polymer liquids. For example, the first column of Fig. 10 shows the shapes of the droplets of polydimethyl siloxane fluid (Fig. 10a), epoxy resin (Fig. 10b), and polybutadiene (Fig. 10c) on the resultant SSM in water. The PCAs of all these polymer droplets are above 150°. The underwater superpolymphobicity enables the SSM to effectively separate the mixtures of water and polydimethyl siloxane fluid (Fig. 10a), epoxy resin (Fig. 10b), and polybutadiene (Fig. 10c), respectively. Therefore, such separation method can be extended to various water/polymer mixtures.

Although the mechanism of the polymer/water separation process is similar to that of oil/water separation based on underwater superoleophobicity, entirely different application conditions are required for these two separation systems. It is more difficult to separate a polymer/water mixture than an oil/water mixture because liquid polymers typically have higher viscosities, lower fluidities, and more complex compositions than pure oils. Using underwater superpolymphobic materials to separate polymer/water mixtures can save polymer resources and prevent polymer-based environmental pollution.

3. Conclusions

In conclusion, micro/nanostructures were easily prepared on the surface of an SSM by fsL processing. After fsL treatment, the SSM was endowed with superhydrophilicity and excellent underwater superpolymphobicity. Liquid PDMS droplets on the structured SSM have a PCA of 156.4 ± 5.1°, a PSA of 2.5 ± 0.5°, and a CAH of 2.7 ± 2° in a water medium. Therefore, fsL processing of the SSM results in high repellence to various liquid polymer droplets. SEM images show that the actual contact between the liquid polymer and the SSM in water is a typical underwater Cassie state. Underwater liquid polymer remains spherical shape on the SSM surface and only contacts the top portion of the SSM microstructure. In addition, underwater superpolymphobicity can be obtained for a laser-treated SSM over a wide range of processing parameters. The laser-induced underwater superpolymphobicity is very stable and the resultant SSM remains its excellent underwater superpolymphobicity after 50 cycles of sandpaper abrasion, strong acid or alkali corrosion for 12 h, UV light irradiation for 24 h, and 40 cycles of tape peeling, respectively. The inverse superhydrophilicity and underwater superpolymphobicity of the

laser-structured SSM were successfully exploited to separate a mixture of a liquid polymer and water with a high separation efficiency and excellent repeatability. The separation efficiency reaches up to 99.0% under a high separation flux of 4.45 × 10^5 L $m^{-2}h^{-1}$. It is demonstrated that the fsL-structured SSM exhibits underwater superpolymphobicity to different liquid polymers and can separate various water/polymer mixtures. This novel strategy for separating polymer/water mixtures has important potential applications for alleviating pollution caused by the discharge of liquid polymers, recycling waste polymer resources, and in polymer production and manufacturing.

4. Experimental section

***Femtosecond laser processing*:** FsL ablation was used to generate microstructures on the SSM surface, thereby changing the wettability of the SSM. As shown in Fig. 1, the SSM (300 mesh size) was fixed on the translation stage in advance. Then, 50-fs laser pulses (center wavelength = 800 nm, repetition rate = 1 kHz) were focused onto the front surface of the SSM via a convex lens (focal length = 20 cm). The SSM was treated using a line-by-line laser scanning method (inset of Fig. 1). The laser power and scanning speed were set at constant values of 300 mW and 5 mm s^{-1}, respectively. The interval (Λ) of the scanning lines was tuned by a program. The ablated SSM was carefully cleaned with alcohol and distilled water.

***Polymer/water separation*:** The mixture of liquid polymers and water was separated by two methods: removal and filtration. Removal was used for a small polymer leak in water. The laser-structured SSM was wetted by water in advance and placed beneath the polymer layer in water. Then, the SSM was pulled up to remove the liquid polymer from the water surface. Filtration was performed using a prewetted structured SSM mounted on a beaker. A mixture of liquid polymer and water (volume ratio of polymer to water = ~1: 4) was poured onto the SSM. Only water penetrated through the structured SSM, while the polymer was intercepted by the SSM. For clear observation, the liquid polymer was dyed red with Oil Red O. The separation of the mixtures of water and various liquid polymers (PDMS, polydimethyl siloxane fluid, epoxy resin, polybutadiene) was carried out. The separation efficiency was calculated by $\eta = m_1/m_0$, where m_1 and m_0 are the mass of the collected polymer and the polymer before separation [44,45]. The separation flux was obtained by making a constant volume of water pass through the structured SSM. The separation flux was calculated by $v = V/(St)$, where V is the water volume, S is the efficient area of the used SSM, and t is the time for water completely passing through.

***Durability evaluation*:** The sandpaper abrasion test was carried out by using sandpaper (1000 mesh) as the friction substrate. The laser-structured SSM with the load of 50 g was placed face-down to the sandpaper and pulled forward for 10 cm for every abrasion cycle. The wettability of the as-prepared SSM after acid or alkali corrosion was measured. The SSM was immersed in the acid or alkali solutions with different pH for 12 h, respectively. The acid or alkali solutions were obtained by diluting phosphoric acid and sodium hydroxide, respectively. The SSM was also irradiated by UV light (wavelength = 365 nm) for different time to investigate the UV resistance. The sample was put below a UV lamp with a distance of 10 cm. For the tape peeling test, a commercially available sticky tape (Deli Group Co., Ltd.) was used to repeatedly paste and peel the SSM surface.

***Characterization*:** The morphology of the SSM surface was observed by a scanning electron microscope (FlexSEM-1000). The XRD analysis was carried out by an Empyrean X-ray diffraction (XRD, PANalytical, Netherlands) with Cu K-alpha1 X-ray source. The wettability of droplets of water and liquid polymer on SSM surfaces was investigated by contact-angle measurement (JC2000D). The main tested liquid polymer was uncured PDMS (DC-184, Dow Corning Corporation). The liquid PDMS was cured by mixing with a curing agent followed by storage at 60 °C for 3 h. In the measurement, a mixture of water and ethanol (V: V = 1: 1) was used as the water environment to ensure that the density of liquid PDMS droplet was higher than that of the water environment.

CRediT authorship contribution statement

Jiale Yong: Conceptualization, Methodology, Writing - original draft, Funding acquisition. **Xue Bai:** Writing - review & editing. **Qing Yang:** Writing - review & editing. **Xun Hou:** Writing - review & editing. **Feng Chen:** Supervision, Project administration, Funding acquisition.

Declaration of Competing Interest

The authors declared that there is no conflict of interest.

Acknowledgments

This work is supported by the National Science Foundation of China under Grant nos. 61805192 and 61875158, the National Key Research and Development Program of China under Grant no. 2017YFB1104700, the International Joint Research Laboratory for Micro/Nano Manufacturing and Measurement Technologies, and the Fundamental Research Funds for the Central Universities.

References

[1] J. Li, R.J. Kuppler, H.-C. Zhou, Selective gas adsorption and separation in metal-organic frameworks, Chem. Soc. Rev. 38 (2009) 1477–1504.
[2] P. Bernardo, E. Drioli, G. Golemme, Membrane gas separation: a review/state of the art, Ind. Eng. Chem. Res. 48 (2009) 4638–4663.
[3] Y.-S. Bae, R.Q. Snurr, Development and evaluation of porous materials for carbon dioxide separation and capture, Angew. Chem. In. Ed. 50 (2011) 11586–11596.
[4] D.-E. Jiang, V.R. Cooper, S. Dai, Porous graphene as the ultimate membrane for gas separation, Nano Lett. 9 (2009) 4019–4024.
[5] A.A. Hyman, C.A. Weber, F. Juelicher, Liquid-liquid phase separation in biology, Annu. Rev. Cell Dve. Bi. 30 (2014) 39–58.
[6] Z. Xue, Y. Cao, N. Liu, L. Feng, L. Jiang, Special wettable materials for oil/water separation, J. Mater. Chem. A 2 (2014) 2445–2460.
[7] J.L. Yong, J. Huo, F. Chen, Q. Yang, X. Hou, Oil/water separation based on natural materials with super-wettability: recent advances, PCCP 20 (2018) 25140–25163.
[8] J.L. Yong, Q. Yang, C.L. Guo, F. Chen, X. Hou, A review of femtosecond laser-structured superhydrophobic or underwater superoleophobic porous surfaces/materials for efficient oil/water separation, RSC Adv. 9 (2019) 12470–12495.
[9] J.L. Yong, Y. Fang, F. Chen, J. Huo, Q. Yang, H. Bian, G. Du, X. Hou, Femtosecond laser ablated durable superhydrophobic PTFE films with micro-through-holes for oil/water separation: Separating oil from water and corrosive solutions, Appl. Surf. Sci. 389 (2016) 1148–1155.
[10] J.L. Yong, F. Chen, Q. Yang, G. Du, C. Shan, J. Huo, Y. Fang, X. Hou, Oil-water separation: a gift from the desert, Adv. Mater. Interfaces 3 (2016) 1500650.
[11] G. Matafonova, V. Batoev, Recent advances in application of UV light-emitting diodes for degrading organic pollutants in water through advanced oxidation processes: a review, Water Res. 132 (2018) 177–189.
[12] V.S. Tran, H.H. Ngo, W. Guo, J. Zhang, S. Liang, C. Ton-That, X. Zhang, Typical low cost biosorbents for adsorptive removal of specific organic pollutants from water, Bioresour. Technol. 182 (2015) 353–363.
[13] E. Lipczynska-Kochany, Humic substances, their microbial interactions and effects on biological transformations of organic pollutants in water and soil: A review, Chemosphere 202 (2018) 420–437.
[14] M. Sajida, M.K. Nazala, N. Baigb Ihsanullaha, A.M. Osmanb, Removal of heavy metals and organic pollutants from water using dendritic polymers based adsorbents: A critical review, Sep. Purif. Technol. 191 (2018) 400–423.
[15] T. Marek, M. Agata, Z. Bogdan, N. Jacek, Green analytical chemistry in sample preparation for determination of trace organic pollutants, Trends Anal. Chem. 28 (2009) 943–951.

[16] P.-F. Idaira, N. Ali, P. Verónica, L.A. Jared, H.A. Juan, M.A. Ana, Utilization of highly robust and selective crosslinked polymeric ionic liquid-based sorbent coatings in direct-immersion solid-phase microextraction and high-performance liquid chromatography for determining polar organic pollutants in waters, Talanta 158 (2016) 125–133.
[17] J. Yong, S.C. Singh, Z. Zhan, E. Mohamed, F. Chen, C. Guo, Femtosecond laser-produced underwater "superpolymphobic" nanorippled surfaces: repelling liquid polymers in water for application of controlling polymer shape and adhesion, ACS Appl. Nano Mater. 2 (2019) 7362–7371.
[18] J. Yong, Z. Zhan, S.C. Singh, F. Chen, C. Guo, Microfludic channels fabrication based on underwater superpolymphobic microgrooves produced by femtosecond laser direct writing, ACS Appl. Polym. Mater. 1 (2019) 2819–2825.
[19] J. Yong, Z. Zhan, S.C. Singh, F. Chen, C. Guo, Femtosecond laser-structured underwater "superpolymphobic" surfaces, Langmuir 35 (2019) 9318–9322.
[20] K. Sugioka, Y. Cheng, Femtosecond laser three-dimensional micro-and nanofabrication, Appl. Phys. Rev. 1 (2014) 041303.
[21] A.Y. Vorobyev, C. Guo, Direct femtosecond laser surface nano/microstructuring and its applications, Laser & Photon. Rev. 7 (2013) 385–407.
[22] K. Sugioka, Y. Cheng, Ultrafast lasers-reliable tools for advanced materials processing, Light Sci. Appl. 3 (2014). e149.
[23] T.C. Chong, M.H. Hong, L.P. Shi, Laser precision engineering: from microfabrication to nanoprocessing, Laser Photon. Rev. 4 (2010) 123–143.
[24] J. Yong, F. Chen, Q. Yang, X. Hou, Femtosecond laser controlled wettability of solid surface, Soft Matter 11 (2015) 8897–8906.
[25] J. Yong, F. Chen, Q. Yang, Z. Jiang, X. Hou, A review of femtosecond-laser-induced underwater superoleophobic surfaces, Adv. Mater. Interfaces 5 (2018) 1701370.
[26] Y. Zhang, Y. Li, Y. Hu, X. Zhu, Y. Huang, Z. Zhang, S. Rao, Z. Hu, W. Qiu, Y. Wang, G. Li, L. Yang, J. Li, D. Wu, W. Huang, C. Qiu, J. Chu, Localized self-growth of reconfigurable architectures induced by a femtosecond laser on a shape-memory polymer, Adv. Mater. 30 (2018) 1803072.
[27] J. Yong, F. Chen, Q. Yang, D. Zhang, U. Farooq, G. Du, X. Hou, Bioinspired underwater superoleophobic surface with ultralow oil-adhesion achieved by femtosecond laser microfabrication, J. Mater. Chem. A 2 (2014) 8790–8795.
[28] J. Yong, Q. Yang, F. Chen, D. Zhang, U. Farooq, G. Du, X. Hou, A simple way to achieve superhydrophobicity, controllable water adhesion, anisotropic sliding, and anisotropic wetting based on femtosecond-laser-induced line-patterned surfaces, J. Mater. Chem. A 2 (2014) 5499–5507.
[29] J. Yong, F. Chen, J. Huo, Y. Fang, Q. Yang, J. Zhang, X. Hou, Femtosecond laser induced underwater superaerophilic and superaerophobic PDMS sheets with through microholes for selective passage of air bubble and further collection of underwater gas, Nanoscale 10 (2018) 3688–3696.
[30] J. Yong, F. Chen, Y. Fang, J. Huo, Q. Yang, J. Zhang, H. Bian, X. Hou, Bioinspired design of underwater superaerophobic and superaerophilic surfaces by femtosecond laser ablation for anti- or capturing bubbles, ACS Appl. Mater. Interfaces 9 (2017) 39863–39871.
[31] J. Yong, F. Chen, M. Li, Q. Yang, Y. Fang, J. Huo, X. Hou, Remarkably simple achievement of superhydrophobicity, superhydrophilicity, underwater superoleophobicity, underwater superoleophilicity, underwater superaerophobicity, and underwater superaerophilicity on femtosecond laser ablated PDMS surfaces, J. Mater. Chem. A 5 (2017) 25249–25257.
[32] J. Yong, S.C. Singh, Z. Zhan, F. Chen, C. Guo, Substrate-independent, fast, and reversible switching between underwater superaerophobicity and aerophilicity on the femtosecond laser-induced superhydrophobic surfaces for selectively repelling or capturing bubbles in water, ACS Appl. Mater. Interfaces 11 (2019) 8667–8675.
[33] X. Bai, Q. Yang, Y. Fang, J. Zhang, J. Yong, X. Hou, F. Chen, Superhydrophobicity-memory surfaces prepared by a femtosecond laser, Chem. Eng. J. 383 (2020) 123143.
[34] J. Yong, J. Huo, Q. Yang, F. Chen, Y. Fang, X. Wu, L. Liu, X. Lu, J. Zhang, X. Hou, Femtosecond laser direct writing of porous network microstructures for fabricating super-slippery surfaces with excellent liquid repellence and anti-cell proliferation, Adv. Mater. Interfaces 5 (2018) 1701479.
[35] Y. Jiao, C. Li, X. Lv, Y. Zhang, S. Wu, C. Chen, Y. Hu, J. Li, D. Wu, J. Chu, In situ tunable bubble wettability with fast response induced by solution surface tension, J. Mater. Chem. A 6 (2018) 20878–20886.
[36] J. Yong, C. Zhang, X. Bai, J. Zhang, Q. Yang, X. Hou, F. Chen, Designing "supermetalphobic" surfaces that greatly repel liquid metal by femtosecond laser processing: does the surface chemistry or microstructure play a crucial role?, Adv. Mater. Interfaces 7 (2020) 1901931.
[37] J. Huo, q. Yang, J. Yong, P. Fan, Y. Lu, X. Hou, F. Chen, Underwater superaerophobicity/superaerophilicity and unidirectional bubble passage based on the femtosecond laser-structured stainless steel mesh, Ad. Mater. Interfaces 7 (2020) 1902128.
[38] J. Yong, F. Chen, Q. Yang, U. Farooq, G. Du, H. Bian, X. Hou, Controllable underwater anisotropic oil-wetting, Appl. Phys. Lett. 105 (2014) 071608.
[39] J. Yong, F. Chen, Q. Yang, J. Huo, X. Hou, Superoleophobic surfaces, Chem. Soc. Rev. 46 (2017) 4168–4217.
[40] S. Wang, L. Jiang, Definition of superhydrophobic states, Adv. Mater. 19 (2007) 3423–3424.
[41] J. Cui, F. Li, Y. Wang, Q. Zhang, W. Ma, C. Huang, Electrospun nanofiber membranes for wastewater treatment applications, Sep. Purif. Technol. 250 (2020) 117116.
[42] M. Zhang, W. Ma, S. Wu, G. Tang, J. Cui, Q. Zhang, F. Chen, R. Xiong, C. Huang, Electrospun frogspawn structured membrane for gravity-driven oil-water separation, J. Colloid Interf. Sci. 547 (2019) 136–144.
[43] W. Ma, M. Zhang, Z. Liu, M. Kang, C. Huang, G. Fu, Fabrication of highly durable and robust superhydrophobic-superoleophilic nanofibrous membranes based on a fluorine-free system for efficient oil/water separation, J. Membrane Sci. 15 (2019) 303–313.
[44] M. Zhang, W. Ma, J. Cui, S. Wu, J. Han, Y. Zhou, C. Huang, Hydrothermal synthesized UV-resistance and transparent coating composited superoleophilic electrospun membrane for high efficiency oily wastewater treatment, J. Hazardous Mater. 383 (2020) 121152.
[45] W. Ma, M. Zhang, Z. Liu, C. Huang, G. Fu, Nature-inspired creation of a robust free-standing electrospun nanofibrous membrane for efficient oil-water separation, Environ. Sci. Nano 5 (2018) 2909–2920.